

Sledgehamr: Simulating Scalar Fields with Adaptive Mesh Refinement

Malte Buschmann*

*GRAPPA Institute, Institute for Theoretical Physics Amsterdam,
University of Amsterdam, Science Park 904, 1098 XH Amsterdam, The Netherlands*

Understanding the non-linear dynamics of coupled scalar fields often necessitates simulations on a three-dimensional mesh. These simulations can be computationally expensive if a large scale separation is involved. A common solution is adaptive mesh refinement which, however, greatly increases a simulation's complexity. In this work, we present `sledgehamr`, an `AMReX`-based code package to make the simulation of coupled scalar fields on an adaptive mesh more accessible. Compatible with both GPU and CPU clusters, `sledgehamr` offers a flexible and customizable framework. While the code had been primarily developed to evolve axion string networks, this framework enables various other applications, such as the study of gravitational waves sourced by the dynamics of scalar fields.

CONTENTS

I. Introduction	1
II. AMR	3
A. Integration scheme	3
B. Tagging cells for refinement	4
C. Local vs global regrid	5
D. Kreiss-Oliger dissipation	7
III. Minimal example	7
A. Implementation	7
B. Compilation and run-time parameters	8
IV. Customizing a new project	9
A. Virtual project functions	9
B. Problem-specific cell tagging	9
C. Modifying truncation error estimates	10
V. Gravitational Waves	10
VI. Simulation Input	11
VII. Simulation Output	11
A. Slices and Volumes	11
B. Truncation Error Estimates	12
C. Projections	12
D. Custom Spectra	12
E. Gravitational Wave Spectra	13
F. Checkpoints	13
G. Custom Output	13
VIII. Discussion	14
Acknowledgments	14
References	14
A. Utility Functions	15
B. List of run-time parameters	15

I. INTRODUCTION

Dynamical systems frequently exhibit complex behavior across different spatial and temporal scales, but often we are able to separate the large-scale dynamics from that at small scales. But this is not always the case: when the microphysics non-trivially affects the macrophysics one cannot disentangle both. This is particularly problematic for non-linear systems where one relies on numerical simulations to study their dynamics. Suddenly we need large simulation volumes to capture the macrophysics but at the same time require high resolution to describe the microphysics correctly. The number of operations needed to evolve those systems can easily exceed our computational capabilities.

Examples of such systems exist plenty, particularly in particle cosmology. The thin walls of expanding vacuum bubbles during a first-order phase transition need to be resolved to correctly determine the spectrum of gravitational waves produced by bubble collision (see e.g. [1–3]). This is extremely challenging in (3+1) dimensions. Axion strings are another example. Axion strings are topological defects of a complex scalar field that appear after spontaneously breaking its underlying $U(1)$ symmetry. They form closed loops with a diameter that is roughly a Hubble length. The width of those axion strings, however, is many orders of magnitude smaller, see Fig. 1 for an illustration. This separation of scales is problematic: We need a simulation volume that is at least a Hubble volume large to fit a single axion string but at the same time need to resolve the much smaller string width to be able to evolve the system in time. Even though this scenario is well motivated and of interest, this has caused progress in understanding the dynamics to be slow and tedious (see for example [4–10] for a few recent simulations of axion strings).

* m.s.a.buschmann@uva.nl

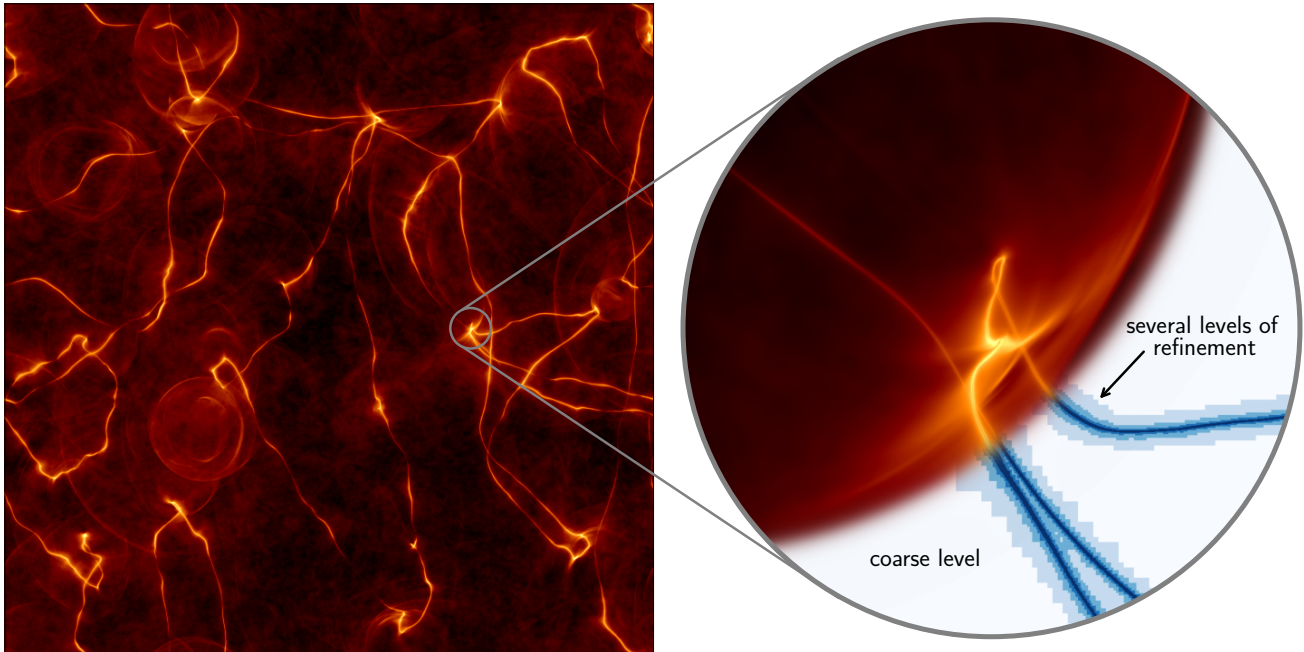


Figure 1. Illustration of axion strings based on a simulation presented in [11] using an older version of `sledgehamr`. The left panel is a 3D→2D projection (sum along the line of sight) of the energy density with a zoom-in in the right panel. Furthermore, the zoom-in shows the underlying refinement level coverage (finest level along the line of sight). In this particular snapshot, the axion string has a diameter of more than five orders of magnitude larger than its width. This makes them an ideal target for AMR simulations since refinement levels concentrated around the string can ensure that the dynamics within the core of the string are properly captured during the evolution without over-resolving the voids between strings.

This paper concerns physics scenarios that can be simulated on a 3-dimensional mesh, in particular systems of coupled scalar fields. Here, there is a well-known approach to alleviate the problem of a large scale separation, *adaptive mesh refinement* (AMR). Rather than having a large mesh with constant grid spacings, with the AMR technique selected parts of the simulation volume will have a higher spatial and temporal resolution than others. This approach works well if the effects of the microphysics are spatially localized. This is the case of axion strings, where high resolution is primarily needed only within the vicinity of the strings.

AMR adds vast amounts of complexity to the simulation which can be a deterrent. Therefore, we present the code package `sledgehamr` (**Sca**Lar **fi**eld **D**ynamics **G**etting **sol**vEd **wit**H **A**daptive **M**esh **R**efinement), with which AMR simulations of coupled scalar fields can be implemented with minimal coding. `sledgehamr` aims to simplify the usage of AMR while still maintaining a large amount of flexibility to adapt to the specific needs of a particular project.

`sledgehamr` uses the `AMReX` software framework [12] internally, a generic AMR library for massively parallel, block-structured applications. As such, `sledgehamr` is scalable with its MPI + tiled OpenMP approach and can run smoothly on both, CPU and GPU clusters. Older

unpublished versions of `sledgehamr` have already been used in a few publications [3, 7, 8, 11] where the code ran on up to 139,264 CPU cores and 1,024 GPUs.

`sledgehamr` solves the (3+1)-dimensional equations of motion (EOMs) of coupled scalar fields with periodic boundary conditions. While the code was originally developed with early universe particle cosmology in mind, it has since undergone an extensive rewrite to accommodate any scenario involving coupled scalar fields. It further provides an interface to co-evolve the tensor perturbations needed to calculate gravitational wave production. Finding convergence criteria to determine which part of the simulation volume should be refined is as much art as it is science. `sledgehamr` employs a data-driven technique using local truncation error estimates to obtain a multi-level AMR grid layout, though other physics-inspired criteria can be implemented as well.

We summarize the AMR terminology and the workflow of `sledgehamr` in section II. A minimal example with a detailed explanation is provided in section III. How a new physics scenario can be implemented in `sledgehamr` from scratch is the topic of section IV with a summary of the gravitational wave framework provided in section V. Section VI and VII describe the simulation input and output, respectively. We conclude in section VIII.

II. AMR

In this section, we want to go over some of the AMR aspects of the code and the general workflow. `sledgehamr` is based on `AMReX`, a software framework for block-structured AMR. As such, the underlying grid is divided into rectangular boxes. To reduce computational overhead the size of each box is always a multiple of the run-time parameter `amr.blocking_factor`. The blocking factor needs to be a power of two and is typically set to 8, 16, or 32 cells. AMR implies we have multiple levels, where each extra refinement level decreases the grid spacing and time step size by a factor of 2. Only the coarse level covers the entire simulation volume whereas each finer level covers parts. How the individual levels are coordinated and advanced in time is described in detail in section II A.

The coarse level grid spacing $\Delta x_{\ell=0} = L/N$ is set by specifying the simulation box length L through `sim.L` and the coarse level grid size N through `amr.coarse_level_grid_size`. The grid spacing Δx_ℓ at level ℓ is then given by

$$\Delta x_\ell = \Delta x_{\ell=0}/2^\ell. \quad (1)$$

The time step size Δt_ℓ is fixed by the Courant-Friedrichs-Lewy condition [13] which dictates

$$\Delta t_\ell/\Delta x_\ell \leq C. \quad (2)$$

C is typically of order one and the ratio $\Delta t_\ell/\Delta x_\ell$ can be set through `sim.cfl`. This subsequently implies the time step size is decreased on each refinement level as well,

$$\Delta t_\ell = \Delta t_{\ell=0}/2^\ell. \quad (3)$$

The refined region is periodically adjusted through a procedure known as *regridding*, hence *adaptive* mesh refinement. Regridding is achieved by checking whether any coarse-level cell should be refined through the concept of cell tagging and then finding a mesh layout that covers all tagged cells. The details of cell tagging are described in section II B. The size of the regrid interval, $\Delta t_{\text{regrid},\ell=0}$, is set by `amr.regrid_dt`. Note that because each refinement level decreases the time step size the regrid interval is also decreased for finer levels,

$$\Delta t_{\text{regrid},\ell} = \Delta t_{\text{regrid},\ell=0}/2^\ell. \quad (4)$$

A. Integration scheme

The integration scheme for an AMR simulation is slightly more complex than a standard fixed-lattice simulation as the various refinement levels need to be coordinated. We illustrate the general workflow for a single coarse-level time step in Fig. 2, both in the time and the spatial domain. We use a simple 1-D simulation with 32

coarse-level cells and two refinement levels as an example though a 3-D simulation works analogously. Furthermore, we use a three-stage integrator, such as a third-order Runge-Kutta scheme, for illustrative purposes but this can be generalized to other integration schemes trivially.

We use a time sub-cycling algorithm to advance the simulation in time, which evolves the individual levels recursively starting at the coarsest. First, the coarse level will be advanced fully regardless of any refinement levels from time t_0 to $t_0 + \Delta t_{\ell=0}$. This implies evolving also regions that are under-resolved by the coarse level. This is intentional, as otherwise, we would introduce non-trivial domain boundaries without a proper expression for the boundary conditions. These under-resolved regions will be corrected at a later stage of the integration.

We can then move on to the next level, $\ell = 1$, by advancing it by $\Delta t_{\ell=1} \equiv \Delta t_{\ell=0}/2$. Here, however, we need to be careful with boundary conditions, since generally, the finer levels will not cover the entire simulation volume. But unlike the coarse level, the fine level has access to the underlying coarse-level data to fill in information outside its domain boundaries. To still be able to compute quantities like field gradients at the domain boundaries we use the concept of *ghost cells*.

Ghost cells are a small number of cells, typically about one or two, that exist on the fine level just outside its domain. Ghost cells are not evolved like the rest of the fine level, instead, they are being interpolated from the underlying coarse level using a 4-th order spatial interpolation scheme. For this to work we need to enforce a gap between coarse/fine boundaries, typically at least one fine-level blocking factor. Without such a gap, we may not be able to set ghost cells at level $\ell = 2$ because the $\ell = 1$ domain might not extend far enough for the interpolation.

Since we need to compute the boundary conditions at every intermediate integration step, ghost cells will need to be set regularly. However, since $\Delta t_{\ell=1} < \Delta t_{\ell=0}$, the coarse-level state does typically not exist for precisely the fine-level time at which we want to compute ghost cells. Therefore, we not only interpolate spatially but also temporally, using the coarse level field state at t_0 and $t_0 + \Delta t_{\ell=0}$. Analogously, level $\ell = 2$ will fill ghost cells from level $\ell = 1$ using the states at t_0 and $t_0 + \Delta t_{\ell=1}$.

Once we recursively advance every level by their respective time step size Δt_ℓ , we can start working backward by evolving the finest level a second time by Δt_ℓ . The state at level ℓ and $\ell - 1$ will now align in time, since $2\Delta t_\ell \equiv \Delta t_{\ell-1}$. This allows us to synchronize both levels, which entails downsampling the fine level to overwrite the underlying coarse-level cells. We also set fine-level ghost cells during this synchronization stage but no temporal interpolation is needed this time. We can also compute truncation error estimates during this synchronization, see section II B.

This procedure can then be repeated until all levels are synchronized at $t_0 + \Delta t_{\ell=0}$.

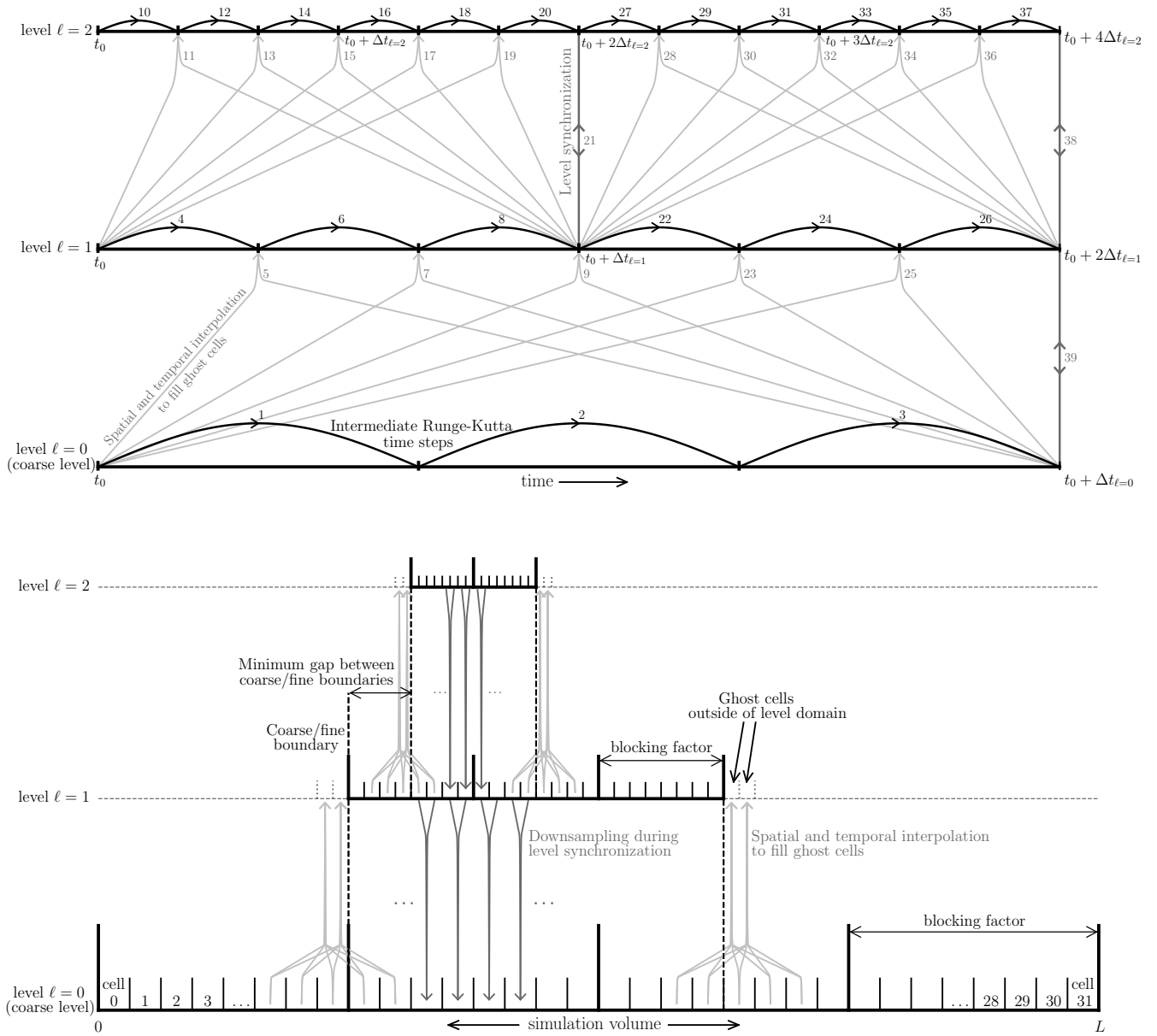


Figure 2. Illustration of the AMR workflow in the time domain (*top*) and the spatial domain (*bottom*) for a 1-D simulation with two refinement levels and 32 coarse-level cells. The simulation advances in time using a recursive *time sub-cycling* algorithm, illustrated above using a three-stage integrator as an example. The numbers in the top panel indicate the order of operation during a single coarse-level time step. These operations consist of (i) the advancement of individual Runge-Kutta steps (1, 2, 3, ...), (ii) the filling of fine-level ghost cells from a coarse level using spatial and temporal interpolation (5, 7, 9, ...) and (iii) the synchronization of two adjacent levels (21, 38, 39). Spatially, each grid is divided into boxes with a size that is a multiple of the *blocking factor*. A small number of ghost cells outside the valid domain of a fine level are filled through interpolation from the coarse level. To ensure proper coverage for this interpolation a gap must exist between coarse/fine boundaries. Coarse-level cells that overlap with fine-level cells are overwritten through an averaging procedure during level synchronization.

B. Tagging cells for refinement

To determine which part of the simulation volume shall be refined we *tag* cells. Every tagged cell will be refined, including a buffer region around it. The size of this buffer

region is set by `amr.n_error_buf`. `sledgehamr` can handle two different types of cell tagging criteria: data-driven and problem-specific.

The data-driven tagging criterion is readily available in `sledgehamr`. The idea is that if one advances identical

states $\phi(x)$ at two different resolutions for a time Δt , the difference between the results,

$$\Delta\phi_{\text{cf}}(x) = |\phi_{\text{coarse}}(x) - \phi_{\text{fine}}(x)|, \quad (5)$$

informs us about their numerical convergence. If $\Delta\phi_{\text{cf}}$ is large the convergence is bad, whereas if the difference is small, both states must have converged reasonably well. We will refer to $\Delta\phi_{\text{cf}}$ as the *truncation error estimate* (TEE). We can use $\Delta\phi_{\text{cf}}$ to identify poorly converging regions in our simulation and tag cells for refinement where $\Delta\phi_{\text{cf}}$ exceeds some threshold ϵ_ϕ .

Of course, this requires us to simulate the same field at two resolutions, but luckily, this comes almost for free in an AMR simulation: A refined level ℓ is always nested within the coarser level $\ell - 1$ and both levels are evolved independently¹ for a time $2\Delta t_\ell = \Delta t_{\ell-1}$ before they are synchronized again. Therefore, we have natural access to TEEs just before synchronization.

This is known as the *self-shadow* method. Obviously, this method breaks down at the coarse level $\ell = 0$ since we would naïvely not co-evolve an even coarser level. To remedy this issue we do indeed introduce such a coarsened version of the coarse level. We dub this the *shadow level* but only introduce it when needed shortly before cell tagging. Once the regrid has been performed the shadow level is removed since we can trivially reconstruct it from the coarse level before the next regrid. The extra computational cost is relatively small since the shadow level is only evolved for a single time step $\Delta t_s = 2\Delta t_{\ell=0}$ once every regridding interval.

We illustrate TEEs in Fig. 3 using a snapshot of a (3+1)-D simulation of a scalar field $\phi(x)$ undergoing a phase transition from the false vacuum at $\phi(x) = 0$ to the true vacuum at $\phi(x) = 1$. Specifically, Fig. 3 shows a slice through two expanding and colliding bubbles of the true vacuum. The exact details of this scenario are not crucial for our illustration but can be found here [3]. In this example, the outer bubble walls are sharp features that require high spatial resolution. This is captured by the fact that TEEs at the bubble walls are large at lower levels due to poor numerical convergence. Subsequently, most of the outer wall is refined down to level $\ell = 3$. Note, however, how the TEE decreases for every extra refinement level until they are ultimately sub-threshold, in this particular case $\epsilon_\phi = 10^{-3}$.

Furthermore, one might notice that there are certain box-like patches separated by a sharp transition where the TEE is larger than in its immediate surroundings. In Fig. 3 this is most obvious on refinement level 1. This is due to an edge effect as this area is right at the boundary of the level domain. In this particular case, level

1 does not extend further into the third dimension in the positive direction. In these boundary cells, gradients appearing in the EOMs are not computed consistently using fine-level data but include ghost cells that are interpolated from the coarse level. The TEEs are therefore larger. This is not an issue, however, as these fine-level TEEs are by construction similar in scale to the TEEs of the coarse level. Since the coarse level TEEs were sub-threshold as otherwise there would be no fine-level domain boundary at this location, the fine-level TEEs will also be sub-threshold.

The TEE threshold ϵ_ϕ can be set through `amr.te_crit`. Furthermore, the actual threshold is implemented as

$$f_\phi(\Delta\phi_{\text{cf}}) > \epsilon_\phi, \quad (6)$$

where $f_\phi(\Delta\phi_{\text{cf}}) = \Delta\phi_{\text{cf}}$ by default. The function $f_\phi(\Delta\phi_{\text{cf}})$ can be changed, however, and we refer to section IV C for implementation details. Besides this data-driven method, it is also possible to implement extra problem-specific criteria to tag cells. How this is done in practice is described in section IV B.

C. Local vs global regrid

One unique aspect of `sledgehamr` we would like to highlight is the difference between *global* and *local* re-grids. The `AMReX` framework provides a regridding method where cells are tagged for refinement and then a Berger-Rigoutsos clustering algorithm is applied to determine the optimal grid layout that encompasses all tagged cells. We refer to this technique as *global* regrid as it clusters all tagged cells globally. A *global* regrid is sufficient in many use cases as it provides an optimized load-balanced grid within a reasonable amount of computing time.

There are, however, cases where a *global* regrid can become a computational bottleneck. For very large simulation volumes, such as those in [11], the grid has to be chopped into an enormous amount of smaller boxes. Determining the optimal layout in this case can take a significant amount of computing time. `sledgehamr` provides a faster alternative to the *global* regrid which we will refer to as a *local* regrid.

During a *local* regrid, cells will be tagged for refinement as usual. However, rather than clustering them to determine a new grid layout, a *local* regrid will leave the existing grid as is. Instead, it identifies tagged cells that are too close to coarse/fine boundaries and simply expands the existing grid around them if needed. Here, it is assumed that any feature cannot travel further than `n_error_buf` cells in between regrids and a cell is therefore considered too close to a grid boundary if it is closer than `n_error_buf` cells. As this entails mostly local operations the algorithm could be parallelized more effectively and thus speed up the regrid.

¹ Except at the boundary region of level ℓ since ghost cells on level ℓ will be spatially and temporally interpolated from $\ell - 1$ at each intermediate integrator step. This correlates level ℓ and $\ell - 1$ which will be noticeable when computing $\Delta\phi_{\text{cf}}$ at these locations.

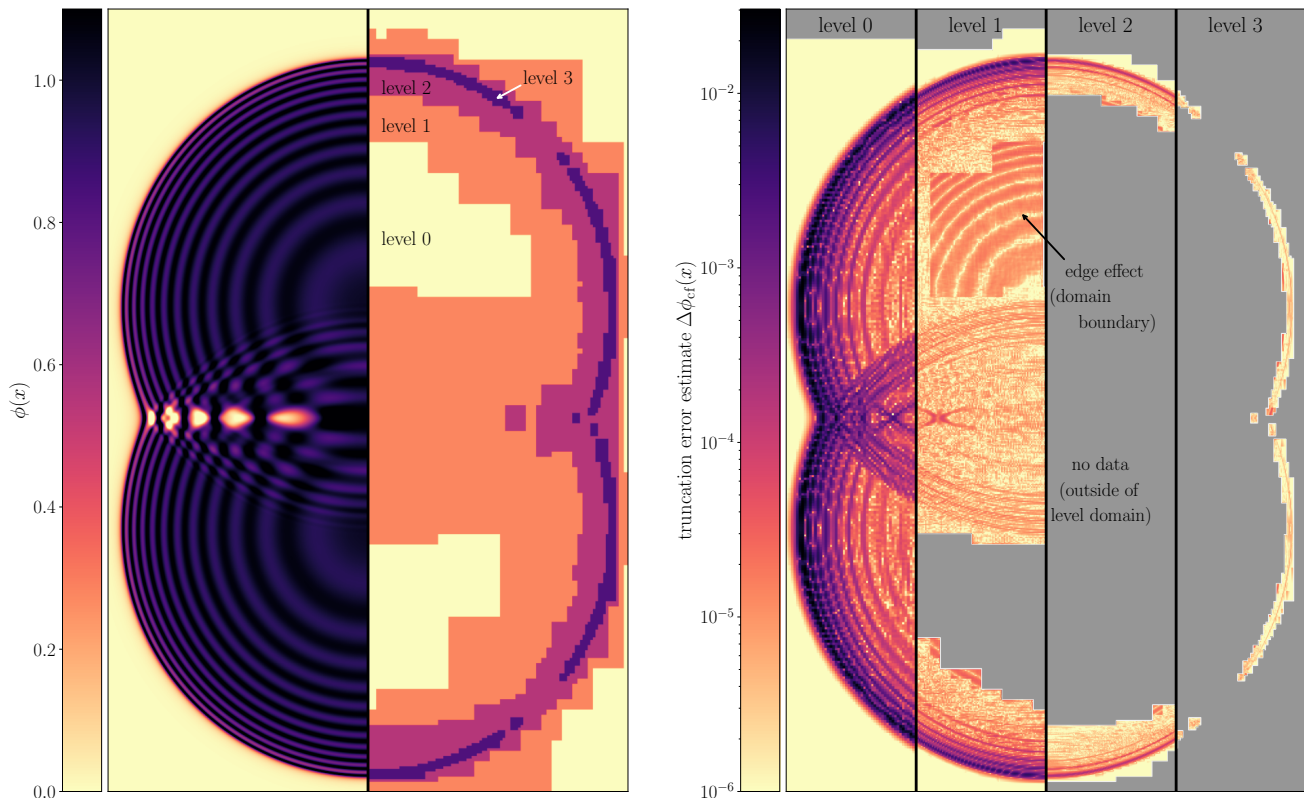


Figure 3. An example of truncation error estimates is illustrated using a slice through a 3-D volume. For details of the simulation see main text. (Left) Slice through one of the scalar field $\phi(x)$ on the left-hand side, and the respective refinement level coverage on the right-hand side. (Right) Corresponding truncation error estimates $\Delta\phi_{cf}(x)$ for all four levels. Gray areas contain no data as this part of the simulation volume is not covered by the respective level.

This algorithm is particularly efficient if the majority of features that require refinement travel slower than their theoretical maximum. For example, in the case of axion strings, any string segment could theoretically move as fast as the speed of light, and near relatively rare string reconnections they will indeed saturate that limit [7, 11]. This forced the conservative choice of a rather large buffer region `n_error_buf` to ensure even the fastest string segment would not be able to leave the refined grid. However, the majority of string segments will move much slower and as such are surrounded by a far larger buffer region than it needs to be. During a local regrid, it will take several regridding intervals for most string segments to get close enough to the grid boundary to trigger extra refinement. This means much of the grid will stay untouched during a local regrid for several regridding intervals. In [11], a local regrid took a few seconds compared to a few minutes for the global regrid, alleviating the bottleneck.

It is important to note that the local regrid comes with several drawbacks despite it being incredibly fast. Most importantly, it only ever increases the refined area and never removes any. Therefore, the local regrid can only ever be used in conjunction with an occasional global regrid to reoptimize the grid layout.

Fortunately, the local regrid module has a built-in logic to automatically determine when a global regrid should be performed instead of a local regrid. It does that by keeping track of how much extra volume has been added by all local regrids since the last global regrid. If this fraction dV_ℓ exceeds some threshold ϵ_s on any refinement level ℓ , it requests a global regrid at the next opportunity starting at the lowest level where $dV_\ell \geq \epsilon_w$. Typically, we have $\epsilon_w < \epsilon_s$ to avoid lower levels triggering a global regrid when higher refinement levels were globally regridded just a moment prior. By default, we have $\epsilon_s = 10\%$ and $\epsilon_w = 5\%$, though these can be adjusted in the inputs file through `amr.volume_threshold_strong = ϵ_s` and `amr.volume_threshold_weak = ϵ_w` . Furthermore, the maximum number of consecutive local regrids without a global regrid can be capped by setting `amr.max_local_regrids`.

There is one more difference between a global and a local regrid that we would like to highlight. If a global regrid is performed at level ℓ , the current AMReX implementation will only modify level ℓ and higher. Coarser levels will be left untouched. This can become an issue at times as level ℓ needs to be always nested within level $\ell - 1$ with at least a `blocking_size`'d wide gap between the boundary of level $\ell - 1$ and the boundary of level ℓ .

If a cell too close to the boundary of level $\ell - 1$ is tagged the algorithm will not be able to refine this cell or otherwise it will violate nesting requirements. This caveat is not present in a local regrid. Here, if a local regrid is performed at level ℓ , the algorithm will also expand lower levels solely to ensure nesting.

D. Kreiss-Oliger dissipation

AMR mixes grids of different resolutions which can be prone to numerical instabilities introduced by the finite-difference method at the respective level boundaries. This can manifest, e.g., through spurious high-frequency modes though the severity is highly problem-specific. In cases where these artifacts become a concern, a common mitigation strategy is the introduction of an extra artificial dissipation term. `sledgehamr` implements Kreiss-Oliger dissipation [14] by adding the small-scale operator

$$Q_\ell = (-1)^{\frac{p+3}{2}} \epsilon_{\text{KO}} \frac{\Delta x_\ell^p}{2^{p+1}} \left(\frac{\partial^{(p+1)}}{\partial x^{(p+1)}} + \frac{\partial^{(p+1)}}{\partial y^{(p+1)}} + \frac{\partial^{(p+1)}}{\partial z^{(p+1)}} \right) \quad (7)$$

to the evolution of each scalar field component. Here, Δx_ℓ is the grid spacing at level ℓ , p is the dissipation order, $\partial^{(p+1)}/\partial x^{(p+1)}$ is the $(p+1)$ -st spatial derivative, and ϵ_{KO} is the overall dissipation strength. Kreiss-Oliger dissipation can be switched on by setting the order p through `sim.dissipation_order` and the strength ϵ_{KO} through `sim.dissipation_strength`.

III. MINIMAL EXAMPLE

A. Implementation

In this chapter, we illustrate how `sledgehamr` can be used to simulate a simple physics scenario with AMR. We use axion strings as an example, which require us to simulate a complex scalar field Φ with the Lagrangian

$$\mathcal{L} = |\partial\Phi|^2 - \left(|\Phi|^2 - \frac{f_a}{2} \right)^2 - \frac{T^2}{3} |\Phi|^2. \quad (8)$$

From this Lagrangian, we can derive the EOMs for the two (dimensionless) components of $\Phi = \frac{f_a}{\sqrt{2}}(\psi_1 - i\psi_2)$ which yields

$$\psi_i'' + \frac{2}{\eta} \psi_i' - \nabla^2 \psi_i + \eta^2 \psi_i (\psi_1^2 + \psi_2^2 - 1) + a \psi_i = 0. \quad (9)$$

Here, η is (comoving) time, ∇^2 is the Laplace operator, and a is some constant. See [7] for more details and derivations. The primes indicate derivatives with respect to η , hence we are dealing with two coupled second-order differential equations. We will further decompose

both second-order equations into four first-order equations. We then have a total of four scalar degrees of freedom, ψ_1 and ψ_2 , and their conjugate momenta $\Pi_1 \equiv \psi_1'$ and $\Pi_2 \equiv \psi_2'$ with respective EOMs

$$\psi_i' = \Pi_i, \quad (10)$$

and

$$\Pi_i' = -\frac{2}{\eta} \Pi_i + \nabla^2 \psi_i - \eta^2 \psi_i (\psi_1^2 + \psi_2^2 - 1) - a \psi_i. \quad (11)$$

To simulate this set of four equations using `sledgehamr` we need to first start a new project by creating a header file `MinimalExample.h` inside the folder `sledgehamr/projects/MinimalExample/`. We chose `MinimalExample` for our project name, but this could have been anything as long as the header file name matches the folder it is contained in. `MinimalExample.h` then consists of the following code:

```

1 #pragma once
2 #include <sledgehamr.h>
3 namespace MinimalExample {
4
5 SLEDGEHAMR_ADD_SCALARS(Psi1, Psi2)
6 SLEDGEHAMR_ADD_CONJUGATE_MOMENTA(Pi1, Pi2)
7
8 AMREX_GPU_DEVICE AMREX_FORCE_INLINE
9 void Rhs(
10     const amrex::Array4<double>& rhs,
11     const amrex::Array4<const double>& state,
12     const int i, const int j, const int k,
13     const int lev, const double time,
14     const double dt, const double dx,
15     const double* params) {
16
17     // Fetch field values.
18     double Psi1 = state(i, j, k, Scalar::Psi1);
19     double Psi2 = state(i, j, k, Scalar::Psi2);
20     double Pi1 = state(i, j, k, Scalar::Pi1);
21     double Pi2 = state(i, j, k, Scalar::Pi2);
22     double eta = time;
23
24     // Compute Laplacians.
25     constexpr int order = 2;
26     double laplacian_Psi1 =
27         sledgehamr::utils::Laplacian<order>(
28             state, i, j, k, Scalar::Psi1, dx*dx);
29     double laplacian_Psi2 =
30         sledgehamr::utils::Laplacian<order>(
31             state, i, j, k, Scalar::Psi2, dx*dx);
32
33     // Compute potential.
34     const int a = 0.56233;
35     double pot =
36         eta*eta*(Psi1*Psi1 + Psi2*Psi2 - 1) + a;
37
38     // Now compute the EOMs.
39     rhs(i, j, k, Scalar::Psi1) = Pi1;
40     rhs(i, j, k, Scalar::Psi2) = Pi2;
41     rhs(i, j, k, Scalar::Pi1) =
42         -Pi1*2./eta + laplacian_Psi1 - Psi1*pot;
43     rhs(i, j, k, Scalar::Pi2) =
44         -Pi2*2./eta + laplacian_Psi2 - Psi2*pot;
45 }
46
47 SLEDGEHAMR_FINISH_SETUP

```

```

48 class MinimalExample
49     : public sledgehamr::Sledgehamr {
50 public:
51     SLEDGEHAMR_INITIALIZE_PROJECT(MinimalExample)
52 };
53
54 }; // namespace

```

This code is all that is required to simulate action strings on an adaptive mesh using `sledgehamr`. The first three lines consist of the standard header guard, an `#include` statement, and the beginning of a namespace. It is crucial to encapsulate our entire project code within a namespace that matches our project name to avoid unwanted conflicts with other projects. We then use the `SLEDGEHAMR_ADD_SCALARS` and `SLEDGEHAMR_ADD_CONJUGATE_MOMENTA` macros to name the fields we want to simulate, in our case $\psi_{1,2}$ and $\Pi_{1,2}$. These macros will set the symbols `Scalar::Psi1`, etc, which we will use to access individual field components later on.

Next, we have the opportunity to define *kernel functions*. Kernel functions are functions that operate on a single grid cell and are thus called numerous times during a simulation. If GPU support is enabled during compilation kernel functions will be executed on GPUs. There is only one kernel function that has to be defined in each project and it is the `Rhs` function. As its name suggests, its purpose is to compute the right-hand side of the EOMs. There exist other optional kernel functions that modify the behavior of `sledgehamr` but those are discussed in section IV.

The `Rhs` function has various function arguments from which the EOMs can be computed. First, we have the two containers `rhs` and `state`. `state` contains the current field state whereas `rhs` is to be filled with the final result of the right-hand side of the EOMs in Eq. (10) and (11). The indices i , j , and k are the cell indices for which we want to compute the EOMs. `state` will only contain valid field values at this particular cell, as well as neighboring cells up to a distance defined by the runtime parameter `amr.n_ghost_cells`. This way `state` will contain just enough information to compute the local field gradients that appear in the EOMs.

Other function arguments include the current refinement level `lev`, current simulation time `time`, time step size `dt`, and grid spacing `dx`. In addition, there is the option to pass other problem-specific parameters to this function, as described in section IV A. Those would be available through `params`, however, in this particular example, we do not need to use this functionality.

In the function body, we compute the EOMs by first fetching all field values at our cell from the `state` container. We then determine the laplacians $\nabla^2\psi_{1,2}$ using one of the `sledgehamr` utility functions (see appendix A). Here, `order` describes how many neighboring cells in each direction should be used during the calculation. Therefore, `order` must always be smaller or equal to the number of ghost cells. We then simply save the final result by setting the values of the `rhs` container for all four field

components according to Eq. (10) and (11).

We finish our project by introducing a derived class `MinimalExample`, where, again, its name must match our project name. The macro `SLEDGEHAMR_FINISH_SETUP` between kernel functions and class declaration together with the macro `SLEDGEHAMR_INITIALIZE_PROJECT($ProjectName)` within the class body ensures that our project is properly linked with `sledgehamr`. The class `MinimalExample` is empty in our particular example and seems of little use. However, its base `sledgehamr::Sledgehamr` contains various virtual functions that can be overridden to customize the simulation workflow. More on this in section IV.

B. Compilation and run-time parameters

We are now ready to compile our project using a makefile such as

```

1 AMREX_HOME      ?= /path/to/AMReX
2 SLEDGEHAMR_HOME ?= /path/to/sledgehamr
3
4 COMP            = gnu
5 USE_CUDA        = TRUE
6
7 include $(SLEDGEHAMR_HOME)/Make.sledgehamr

```

and executing `make -j 6`. In this makefile we provide file paths to the `AMReX` and `sledgehamr` GitHub repositories, define a compiler environment, and whether we want to compile with GPU support. The created binary can then be run using, e.g., `srun`. Often something like this will work but your mileage may vary depending on your system architecture:

```

1 export SLURM_CPU_BIND="cores"
2 export OMP_PLACES=threads
3 export OMP_PROC_BIND=spread
4 export OMP_NUM_THREADS=16
5 srun main3d.gnu.MPI.OMP.CUDA.ex inputs

```

In this particular case, `sledgehamr` was compiled with MPI, OpenMP, and CUDA support. Note how the executable expects a file called `inputs`. This file will contain all run-time parameters such as start and end time, grid size, box length, and much more. For example:

```

1 # ----- Select project
2 project.name = MinimalExample
3
4 # ----- Simulation parameters
5 sim.t_start = 0.1
6 sim.t_end   = 5.5
7 sim.L       = 15
8 sim.cfl     = 0.3
9
10 # ----- Integrator
11 integrator.type = 10
12
13 # ----- AMR parameters
14 amr.coarse_level_grid_size = 256
15 amr.blocking_factor       = 8
16 amr.nghost                = 2
17 amr.max_refinement_levels = 2

```



```

18 amr.n_error_buf      = 3
19 amr.regrid_dt       = 0.2
20
21 amr.te_crit = 1e-2
22
23 # ----- Input parameters
24 input.initial_state = initial_state.hdf5
25
26 # ----- Output settings
27 output.output_folder = output
28 output.slices.interval = 0.5
29 output.coarse_box.interval = 3

```

A full list of all input parameters including an explanation can be found in appendix B. The `sledgehamr` GitHub repository provides a README and a Jupyter notebook with detailed instructions for how to compile, run, and analyze the example.

IV. CUSTOMIZING A NEW PROJECT

This chapter is about how one can start a new project and customize the simulation workflow to adapt to the problem-specific needs of the project.

The easiest way to start a new project from scratch is to create a copy of the `MinimalExample` folder under `sledgehamr/projects/` and replace every instance of `MinimalExample` with the new project name. And that is it. `sledgehamr` will automatically detect that a new project has been created and will include it the next time it is compiled.

Besides the obvious modifications such as changing the number of field components in the `SLEDGEHAMR_ADD_SCALARS` and `SLEDGEHAMR_ADD_CONJUGATE_MOMENTA` macro calls, and adapting the EOMs in the `Rhs` kernel function various other options exist to change the simulation workflow. These modifications are typically done either through (i) the implementation of specific kernel functions or (ii) through overriding virtual functions of the project class. Several of these techniques are demonstrated in the `NextToMinimalExample` provided with the GitHub repository.

A. Virtual project functions

The project class is a class derived from `sledgehamr::Sledgehamr`, as seen in the example in section III. As such it does not only inherit access to the raw data through member functions such as `GetLevelData(const int lev)`² but can also modify the workflow through the overriding of virtual functions.

² For a full list of available functions see <https://msabuschmann.github.io/sledgehamr/>

The most commonly overridden virtual function is `void Init()`, which will be called at the end of the initialization phase. Here, we could perform extra modifications to the initial state, parse project-specific input parameters from the `inputs` file using `amrex::ParmParse`, or even add extra custom output types (see section VIIG).

Another useful virtual function is

```

1 void SetParamsRhs(
2     std::vector<double>& params,
3     const double time, const int lev)

```

which gives us access to an empty `params` vector. We can fill this vector with data that will then become accessible in the `Rhs` kernel function through the `const double* params` argument. `SetParamsRhs` will be called before every time step, so `params` can be filled with time-dependent data.

A common use case would be constants in the EOMs. For example, we could add a new parameter `c` to the `inputs` file, `project.c = 1`, and parse this parameter in the `Init()` function through

```

1 amrex::ParmParse pp("project");
2 pp.get("c", c);

```

By then adding `c` to the `params` vector using `params.push_back(c)` in the `SetParamsRhs` function we can fetch it in the `Rhs` kernel function through `double c = params[0]`.

Further virtual functions at our disposal are

```

1 bool CreateLevelIf(const int lev,
2                   const double time);
3 bool StopRunning(const double time);
4 void BeforeTimestep(const double time);

```

The `CreateLevelIf` function is an extra criterion for whether we want to introduce a refinement level $\ell = \text{lev}$. By default, any refinement level is allowed to be created at any time, however, with this virtual function we could delay its creation based on some problem-specific measure. Similarly, `StopRunning` allows us to override the stopping criterion of the simulation, which by default is $t \geq t_{\text{end}}$. Lastly, `BeforeTimestep` is a function that will be executed before every coarse-level time step. Its function is versatile and could be, for example, used to update auxiliary data periodically.

B. Problem-specific cell tagging

Occasionally, tagging individual cells for refinement through TEEs might not be sufficient or we merely want to complement it with some other criterion. A problem-specific tagging criterion can be added to a project by simply defining the following kernel function:

```

1 template<>
2 AMREX_GPU_HOST_DEVICE AMREX_FORCE_INLINE
3 bool TagCellForRefinement<true>(
4     const amrex::Array4<const double>& state,
5     const int i, const int j, const int k,

```

```

6  const int lev, const double time,
7  const double dt, const double dx,
8  const double* params) {
9  \ \ return true or false ...
10 }

```

Each function argument is analog to those of the `Rhs` kernel and the `params` argument can be set by overriding the corresponding virtual `SetParamsTagCellForRefinement` function. Nothing else needs to be done³ as long as this kernel function definition is added to the correct space in between the `SLEDGEHAMR_ADD_CONJUGATE_MOMENTA` and `SLEDGEHAMR_FINISH_SETUP` macro calls, see the example in section III. Cell tagging through TEEs can be used simultaneously and a cell will be tagged if either of the two methods tags it.

C. Modifying truncation error estimates

Cells on level ℓ are tagged for refinement through TEEs if

$$f_\phi(\Delta\phi_{\text{cf},\ell}) > \epsilon_\phi, \quad (12)$$

where $\Delta\phi_{\text{cf},\ell}(x) = |\phi_\ell(x) - \phi_{\ell-1}(x)|$ is the difference of the scalar field $\phi(x)$ between the coarse level $\ell - 1$ and fine level ℓ after evolving them independently for $2\Delta t_\ell \equiv \Delta t_{\ell-1}$. By default, we have $f_\phi(\Delta\phi_{\text{cf}}) = \Delta\phi_{\text{cf}}$ and ϵ_ϕ can be set in the `inputs` file through `amr.te_crit.phi` (or `amr.te_crit` for all scalar field components simultaneously). The function $f_\phi(\Delta\phi_{\text{cf}})$ can be modified by adding the following kernel function:

```

1  template<>
2  AMREX_GPU_HOST_DEVICE AMREX_FORCE_INLINE
3  double TruncationModifier<Scalar::phi>(
4      const amrex::Array4<const double>& state,
5      const int i, const int j, const int k,
6      const int lev, const double time,
7      const double dt, const double dx,
8      const double truncation_error,
9      const double* params) {
10     \ \ return f_\phi(\Delta\phi_{cf})
11 }

```

Note that this is an explicit template specialization for `Scalar::phi`, so we can implement a different function for each scalar field component separately. All function arguments are analog to the `Rhs` kernel function, with the addition of `truncation_error` $\equiv \Delta\phi_{\text{cf}}(x)$.

Similarly, just like for the `Rhs` kernel function, we can set `params` through the function `SetParamsTruncationModifier`. This can be particularly useful as $\Delta\phi_{\text{cf}}$ is an absolute quantity and thus overall field amplitude might matter. One could use `SetParamsTruncationModifier` to compute, for example, a standard deviation and pass it through `params` to normalize $\Delta\phi_{\text{cf}}$ to the TEE threshold ϵ_ϕ .

³ The above code snippet is technically a template specialization thus it will be automatically integrated.

V. GRAVITATIONAL WAVES

The motivation for studying the evolution of coupled scalar fields is often the gravitational waves sourced by their dynamics. In `sledgehamr`, it is possible to simulate gravitational wave production relatively easily, we simply need to toggle them on with `sim.gravitational_waves=1` and provide the corresponding EOMs. Here, we use the auxiliary field method [15] where the transverse-traceless gauge-invariant metric perturbation h_{ij} are evolved through auxiliary fields u_{ij} . Both are related through

$$h_{ij}(t, \mathbf{k}) = \Lambda_{ij,lm}(\mathbf{k})u_{ij}(t, \mathbf{k}) \quad (13)$$

where the object $\Lambda_{ij,lm}$ is constructed from the projector

$$P_{ij}(\mathbf{k}) = \delta_{ij} - \hat{k}_i^{\text{eff}}\hat{k}_j^{\text{eff}} \quad (14)$$

with the effective lattice momentum \hat{k}_i^{eff} as

$$\Lambda_{ij,lm}(\mathbf{k}) = P_{il}(\mathbf{k})P_{jm}(\mathbf{k}) - \frac{1}{2}P_{ij}(\mathbf{k})P_{lm}(\mathbf{k}). \quad (15)$$

The exact definition of \hat{k}_i^{eff} depends on the simulation details, see section VIII E for further details. Typically, the EOMs in configuration space can then be expressed as

$$\ddot{u}_{ij} + 3H\dot{u}_{ij} - \frac{1}{a^2}\nabla^2 u_{ij} = 16\pi GT_{ij}, \quad (16)$$

where H is the Hubble rate, a the scale factor, T_{ij} the stress-tensor sourcing the gravitational waves, and G the gravitational constant. Since the explicit form of Eq. 16 is problem-specific the EOMs have to be implemented for each project separately. This, however, can be done easily by adding the kernel function

```

1  template<>
2  AMREX_GPU_DEVICE AMREX_FORCE_INLINE
3  void GravitationalWavesRhs<true>(
4      const amrex::Array4<double>& rhs,
5      const amrex::Array4<const double>& state,
6      const int i, const int j, const int k,
7      const int lev, const double time,
8      const double dt, const double dx,
9      const double* params) {
10     \ \ Compute Rhs of EoM here ...
11 }

```

The procedure here is precisely the same as for the `Rhs` kernel function, except now for the auxiliary field u and its conjugate momenta \dot{u} . The objects `rhs` and `state` will now not only include the usual scalar field components but also the auxiliary fields. Where the scalar field components can be accessed through `Scalar::MyScalar`, the auxiliary fields u and \dot{u} can be accessed with `Gw::u_${i}$j` and `Gw::du_${i}$j`, respectively. Here, `_${i}$j` is short for the six degrees of freedom `xx`, `yy`, `zz`, `xy`, `xz`, and `yz`. Analogously, `params` can be set by overriding the virtual function `SetParamsGravitationalWaveRhs`. The corresponding unbinned gravitational wave spectrum can be computed automatically, see section VII E for details.

VI. SIMULATION INPUT

At the beginning of a simulation, all field components will be initialized to zero, though we typically want to overwrite these with some pre-generated state. To do so, we can save the initial state as a dataset in an hdf5 file and add `input.initial_state = $PathToFile` to the `inputs` file. The name of the dataset should correspond to the name that was given to each scalar in the `SLEDGEHAMR_ADD_SCALARS` and `SLEDGEHAMR_ADD_CONJUGATE_MOMENTA` macros. Alternatively, we can provide a file for each component separately through `input.initial_state.$MyScalar = $PathToFile`, in which case `data` is an acceptable dataset name as well.

For very large simulations with a coarse-level resolution of 2048^3 and larger, it can be beneficial to split up the initial state into chunks rather than providing it in one large file. Here, our strategy is to use one chunk per compute node, so the first step is to determine the proper chunk size and location. This can be done easily by temporarily adding `input.get_box_layout_nodes = #nodes` to the `inputs` file. In the presence of this parameter, `sledgehamr` will not start a simulation but instead write an hdf5 file containing a list of chunk locations.⁴ This list can then be used to prepare the initial state. To feed the initial state into `sledgehamr`, we can set `input.initial_state` to the folder containing the individual chunks. Here, we need to follow the naming convention `$MyScalar.$i.hdf5`, where `$i` is the number of the chunk.

The size of the provided initial state should match that of the coarse level. However, we can provide a downsampled version and use `input.upsample=2` to up-scale the initial state to the coarse-level resolution through interpolation. Any upsample factor that is a power of 2 is acceptable, as long as it is smaller than the blocking factor.

VII. SIMULATION OUTPUT

`sledgehamr` provides various types of output that can be written periodically to a folder set by `output.output_folder` in the `inputs` file. Some of the different output types are described in the following subsections, but they can all be controlled by following the same pattern. Setting `output.*.interval` to a positive floating-point value in the `inputs` file will allow the output to be written in regular intervals. We can also set a minimum (maximum) time before (after) which no output will be written. This is controlled by `output.*.min_t` (`output.*.max_t`). Here, the asterisk corresponds to the output types, which are:

- checkpoints
- slices
- coarse_box
- full_box
- slices_truncation_error
- coarse_box_truncation_error
- full_box_truncation_error
- projections
- spectra
- gw_spectra
- performance_monitor
- amrex_plotfile

These different types are explained in the next few sections.

Sometimes, certain output types can take up a significant amount of disk space. To help distribute disk usage we can define an alternative output folder through `output.alternative_output_folder`. If for any output type `output.*.alternate` is set to 1 then every second output of this type will be written in the alternative output folder location rather than the primary.

An interface to easily write problem-specific custom output is provided as well, see section VII G. Other parameters to control the output behavior can be found in appendix B. We also provided the python-based tool `pySledgehamr` to easily read and visualize the different outputs. To use `pySledgehamr` we simply need to create an instance of the output class:

```
1 import sys
2 sys.path.append(PathToSledgehamrDirectory)
3 import pySledgehamr as sl
4 output = sl.Output(PathToOutputDirectory)
```

The object `output` can then be used to load the simulation output, the details of which are explained in the following.

A. Slices and Volumes

There are three different output types that directly output the field state of all scalar components: `slices`, `coarse_box`, and `full_box`. `slices` will output three slices through the field at $x = 0$, $y = 0$, and $z = 0$, respectively. If part of the slice has been refined these higher levels will be written to disk as well. `coarse_box` simply writes the entire coarse-level field state. By setting `output.coarse_box.downsample_factor` to any power of 2^5 we can write a downsampled version

⁴ In this case, `sledgehamr` can be run on a single core as no major memory will be allocated.

⁵ Must be \leq `amr.blocking_factor`.

of the coarse box to save disk space. Similarly, `full_box` will write the entire field state but unlike `coarse_box` it will include all refinement levels. Also here, we can produce a downsampled version by setting `output.full_box.downsample_factor` appropriately.

To load the result we can use `pySledgehamr`:

```
1 output.GetSlice(i, direction, level, fields)
2 output.GetCoarseBox(i, fields)
3 output.GetFullBox(i, level, fields)
```

These functions will load the i -th state at refinement level `level` of all scalar fields included in the list `fields`. Furthermore, `direction` \in {"x", "y", "z"} specifies the orientation of the slices. Each function returns a dictionary containing the corresponding time t and the state of each scalar field.

B. Truncation Error Estimates

One of the main refinement criteria are TEEs described section II B. These can be saved using the output types `slices_truncation_error`, `coarse_box_truncation_error`, and `full_box_truncation_error`. These work completely analogously to `slices`, `coarse_box`, and `full_box`, including the downsampling factors. A version of the corresponding field state is included in the output as well to allow for a direct comparison. Note that the output interval for these output types can be slightly larger than `output.*.interval` as TEEs are only computed during regrids. `sledgehamr` therefore has to wait for a regrid at the coarse level before these output types can be written.

The output can be loaded analogously to normal slices and boxes by adding `TruncationError` to the respective `pySledgehamr` function name.

C. Projections

Particularly useful output types are projections, which are 2-dimensional outputs where the third dimension is integrated out. That way we can visually observe features in the entire simulation volume without having to save the full 3-dimensional output. Projections will also include fine-level data by up-sampling the 2-D output to the resolution of the finest level. The maximum level can be capped through `output.projections.max_level`, however. Restricting the maximum level is recommended, as proper up-sampling to the target resolution can take a significant amount of time.

It is typically not useful to project the field components itself. Instead, projecting a derived quantity like an energy density is often more meaningful. Therefore, we always need to specify how to compute such quantity. To do so we need to define a new kernel function using the following template:

```
1 AMREX_FORCE_INLINE
2 double MyProjection(
3     amrex::Array4<double const> const& state,
4     const int i, const int j, const int k,
5     const int lev, const double time,
6     const double dt, const double dx,
7     const std::vector<double>& params) {
8     // Return my derived quantity...
9 }
```

The function arguments are the same as those of the `rhs` function, see section III, and we need to return the derived quantity at cell (i, j, k) . While `params` in the `rhs` function can be set by overriding `SetParams`, we can do the equivalent here by overriding `SetParamsProjections`. To use this kernel function for a projection all we need to do is add

```
1 io_module->projections.emplace_back(
2     MyProjection, "MyProjection");
```

to the projects `Init` function⁶. Here, the first argument is the name of the kernel function, whereas the second argument is a unique identifying string. Multiple different projection types can be added this way, which will all be computed simultaneously. The projections can be loaded with `pySledgehamr` using `output.GetProjection(i, ["MyProjection"])`.

D. Custom Spectra

It is possible to compute unbinned 1-D spectra of the form

$$S_X(|\mathbf{k}|) = \frac{Lt}{2\pi N^6} \sum_{\mathbf{k}=|\mathbf{k}|} |\tilde{X}(\mathbf{k})|^2, \quad (17)$$

at runtime, where L is the box size, N^3 is the total number of coarse level cells, t the current time, and \tilde{X} is the Fourier transform of a quantity X . X can be defined using the same kernel function template we use for projections, see section VII C. Adding a spectrum type to a project works entirely analogously to a projection as well by simply adding

```
1 io_module->spectra.emplace_back(
2     MySpectrum, "MySpectrum");
```

to the projects `Init` function. All spectra will be computed using the coarse-level information to avoid the usage of a non-uniform FFT scheme.

Note that producing unbinned spectra involves knowing all unique combinations of $i^2 + j^2 + k^2$ for $i, j, k \in [0, N)$. `sledgehamr` will load these combinations from a file to save run-time rather than re-computing them each time. The file provided by the GitHub repository contains all necessary data for coarse-level sizes of up to $N^3 = 1024^3$. For larger coarse

⁶ See section IV A.

levels⁷ the unique combinations need to be added to this file first, which can be done easily by running the notebook `notebooks/AddSpectrumBins.ipynb`. The spectra can be loaded using `output.GetSpectrum(i, ["MySpectrum"])`.

E. Gravitational Wave Spectra

If the simulation is evolved with gravitational waves the corresponding spectrum can be automatically computed by setting `output.gw_spectra.interval` to a positive value. For ultimate flexibility, the output will be the unbinned quantity

$$G(|\mathbf{k}|) = \frac{1}{N^6} \sum_{\mathbf{k}=|\mathbf{k}|} \Lambda_{ij,lm}(\mathbf{k}) \tilde{u}'_{ij}(\mathbf{k}) \tilde{u}^*_{lm}(\mathbf{k}) \quad (18)$$

from which the differential spectrum $\partial\rho_{\text{GW}}/\partial k$ can easily be constructed follow the procedure outlined in [15]. Here, N^3 is the total number of coarse level cells, \tilde{u}'_{ij} is the Fourier transform of the auxiliary field \tilde{u}_{ij} and $\Lambda_{ij,lm}$ is given in Eq. 15. The computation of $\Lambda_{ij,lm}$ requires us to specify the effective lattice momentum \mathbf{k}^{eff} which depends on how the gradients in the auxiliary field source term are computed. We have currently two types implemented which can be selected by setting `output.gw_spectra.projection_type` to either 1 (suitable for 2nd order finite-difference gradients) or 2 (suitable for 4th order finite-difference gradients). The gravitational wave spectrum will be computed based on the coarse level. However, just like for general spectra, this requires pre-computing all unique combinations of $i^2 + j^2 + k^2$ for $i, j, k \in [0, N]$ if the coarse-level is larger than $N^3 = 1024^3$. See section VIII D for details.

Furthermore, it is possible to compute gravitational wave spectra based on a modified version of (18). This can be achieved by deriving a class from the base class `GravitationalWavesSpectrumModifier`, which has two virtual functions that can be overridden to change the $\tilde{u}'_{ij}(\mathbf{k})\tilde{u}^*_{lm}(\mathbf{k})$ term. An instance of this class can then be passed to the routine that computes the gravitational wave spectra, e.g.

```
1 unique_ptr<GravitationalWavesSpectrumModifier>
  modifier = make_unique<MyModification>();
2 gravitational_waves->ComputeSpectrum(hdf5_file,
  modifier.get());
```

as part of a new output type⁸. We abstain from further details here, but a full implementation example can be found in the `FirstOrderPhaseTransition` project that comes with the GitHub repository. The spectra can be loaded using `output.GetGravitationalWaveSpectrum(i)`.

⁷ They are not provided by default to avoid unnecessarily large file sizes.

⁸ See section VIII G

F. Checkpoints

One of the key features of any simulation code of this size are of course checkpoints. Checkpoints allow a simulation to be restarted after an early termination of the program. To periodically write checkpoints one needs to set `output.checkpoints.interval` to a positive value. As checkpoints can take up a significant amount of disk space since they contain data of all levels at full double precision, it is often beneficial to set `output.checkpoints.rolling = 1`. In this case, only the last checkpoint is kept on disk and any older checkpoints are deleted. To restart a simulation from a checkpoint we need to set `input.restart = 1`. `sledgehamr` will automatically find the latest checkpoint within the output folder, although a specific checkpoint can be selected through `input.select_checkpoint`.

G. Custom Output

In addition to the above-mentioned pre-defined output types, it is possible to implement extra problem-specific output. All that is needed is to add

```
1 io_module->output.emplace_back("MyOutput",
  OUTPUT_FCT(MyOutput));
```

to the projects `Init` function. Here, the first argument is a unique string to identify the output type. Through this, all typical input parameters such as `output.MyOutput.interval` become available. The second argument is a function pointer, pointing to a function of the form

```
1 bool MyOutput(double time, std::string prefix) {
2     // Write custom output here
3     // ...
4     return true;
5 }
```

Here the actual writing of the output can be implemented, where the function arguments provide the current time and the folder `prefix` to which the output shall be written. Furthermore, we expect a boolean value as a return indicating whether the writing of the output was successful. If `false` is returned, the folder `prefix` will be deleted and another writing attempt will be performed next interval. If `MyOutput` is a member function of the project class, we can access all level data easily through, e.g., `sim->GetLevelData(lev)`.

Besides custom output, it is also possible to modify the interval at which output is written. Output is written once $f(t_{\text{Current}}) > f(t_{\text{LastWritten}}) + \text{interval}$, where `interval` is set by `output.*.interval`. The default is $f(t) = t$, but this can be modified through

```
1 io_module->output[sim->io_module->idx_*].
2   SetTimeFunction(TIME_FCT(MyF_of_t));
```

where

```
1 double MyF_of_t(const double t) {
```

```

2   return ...
3 }

```

Here, the asterisks in `sim->io_module->idx_*` shall be replaced by the output type for which we want to change $f(t)$, e.g. `sim->io_module->idx_checkpoints`. This also affects the minimum (maximum) time `min_t` (`max_t`), where we have $f(t) > \text{min}_t$.

Concrete examples of custom output implementations and modifications to the write interval can be found in the `AxionStrings` project that comes with the GitHub repository.

VIII. DISCUSSION

We present `sledgehamr`, a massively parallelized GPU-enabled code to simulate an arbitrary amount of coupled scalar fields on an adaptive mesh. `sledgehamr` aims to simplify the use of AMR by balancing usability and complexity. While easy to use it provides a flexible and customizable interface that allows, for example, for the computation of gravitational wave spectra.

`sledgehamr` is still in active development and will

likely be expanded with additional features in the future. Older version, however, have already been used successfully in a few publications [3, 7, 8, 11], which, for example, provide one of the most robust predictions of the QCD axion mass in a post-inflationary scenario [7, 11].

ACKNOWLEDGMENTS

We would like to thank J. Benabou, J. Foster, M. Khe-lashvili, and A. Kunder for having used the code during various stages of its development as well as B. Safdi and W. Zhang for helpful discussions. We acknowledge funding from the European Research Council (ERC) under the European Union’s Horizon 2020 research and innovation programme (Grant agreement No. 864035). This research used resources of the National Energy Research Scientific Computing Center (NERSC), a U.S. Department of Energy Office of Science User Facility located at Lawrence Berkeley National Laboratory, operated under Contract No. DE-AC02-05CH11231 using NERSC award HEP-ERCAP0023978.

-
- [1] Daniel Cutting, Mark Hindmarsh, and David J. Weir, “Gravitational waves from vacuum first-order phase transitions: from the envelope to the lattice,” *Phys. Rev. D* **97**, 123513 (2018), [arXiv:1802.05712 \[astro-ph.CO\]](#).
 - [2] Daniel Cutting, Elba Granados Escartin, Mark Hindmarsh, and David J. Weir, “Gravitational waves from vacuum first order phase transitions II: from thin to thick walls,” *Phys. Rev. D* **103**, 023531 (2021), [arXiv:2005.13537 \[astro-ph.CO\]](#).
 - [3] Malte Buschmann, Joshua W. Foster, Sarah R. Geller, and Toby Opferkuch, “Thick and Thin Wall Collisions with Adaptive Mesh Refinement,” to appear.
 - [4] Marco Gorghetto, Edward Hardy, and Giovanni Villadoro, “Axions from Strings: the Attractive Solution,” *JHEP* **07**, 151 (2018), [arXiv:1806.04677 \[hep-ph\]](#).
 - [5] Marco Gorghetto, Edward Hardy, and Giovanni Villadoro, “More Axions from Strings,” *SciPost Phys.* **10**, 050 (2021), [arXiv:2007.04990 \[hep-ph\]](#).
 - [6] Marco Gorghetto, Edward Hardy, and Horia Nicolaescu, “Observing invisible axions with gravitational waves,” *JCAP* **06**, 034 (2021), [arXiv:2101.11007 \[hep-ph\]](#).
 - [7] Malte Buschmann, Joshua W. Foster, Anson Hook, Adam Peterson, Don E. Willcox, Weiqun Zhang, and Benjamin R. Safdi, “Dark matter from axion strings with adaptive mesh refinement,” *Nature Commun.* **13**, 1049 (2022), [arXiv:2108.05368 \[hep-ph\]](#).
 - [8] Joshua N. Benabou, Malte Buschmann, Soubhik Kumar, Yujin Park, and Benjamin R. Safdi, “Signatures of primordial energy injection from axion strings,” *Phys. Rev. D* **109**, 055005 (2024), [arXiv:2308.01334 \[hep-ph\]](#).
 - [9] Ken’ichi Saikawa, Javier Redondo, Alejandro Vaquero, and Mathieu Kaltschmidt, “Spectrum of global string networks and the axion dark matter mass,” (2024), [arXiv:2401.17253 \[hep-ph\]](#).
 - [10] Heejoo Kim, Junghyeon Park, and Minho Son, “Axion Dark Matter from Cosmic String Network,” (2024), [arXiv:2402.00741 \[hep-ph\]](#).
 - [11] Joshua N. Benabou, Malte Buschmann, Joshua W. Foster, and Benjamin R. Safdi, “Axion Mass Prediction from adaptive mesh refinement cosmological lattice simulations,” to appear.
 - [12] Weiqun Zhang, Ann Almgren, Vince Beckner, John Bell, Johannes Blaschke, Cy Chan, Marcus Day, Brian Friesen, Kevin Gott, Daniel Graves, Max Katz, Andrew Myers, Tan Nguyen, Andrew Nonaka, Michele Rosso, Samuel Williams, and Michael Zingale, “AMReX: a framework for block-structured adaptive mesh refinement,” *Journal of Open Source Software* **4**, 1370 (2019).
 - [13] R. Courant, K. Friedrichs, and H. Lewy, “Über die partiellen Differenzgleichungen der mathematischen Physik,” *Math. Ann.* **100**, 32–74 (1928).
 - [14] H. Kreiss and J. Oliger, “Methods for the Approximate Solution of Time,” *Dependant Problems (GARP Publication Series no 10)* (1973).
 - [15] Daniel G. Figueroa, Juan Garcia-Bellido, and Arttu Rajantie, “On the Transverse-Traceless Projection in Lattice Simulations of Gravitational Wave Production,” *JCAP* **11**, 015 (2011), [arXiv:1110.0337 \[astro-ph.CO\]](#).

Appendix A: Utility Functions

Every non-trivial equation of motion contains some spatial operator such as the gradient operator ∇ or the Laplace operator $\Delta \equiv \nabla^2$. `sledgehamr` provides utility functions for the most common versions ready to be used inside kernel functions. In section III we have already seen an example for the Δ operator:

```
1 constexpr int order = 2;
2 double Laplacian_Psi1 = sledgehamr::utils::Laplacian<order>(state, i, j, k, Scalar::Psi1, dx*dx);
```

The function arguments should be self-explanatory given the context. The Δ operator is calculated through the finite difference method and `order` defines the stencil size. Explicitly, `order` corresponds to the number of ghost cells required for the computation, *i.e.* `order`=1, 2, 3 corresponds to the 7-, 13-, 19-point stencil. Note that we want `order` to be a `constexpr` as this allows the compiler to always inline the utility function. This will avoid potentially costly function call overhead within the kernel function. For the Δ operator we have implementations for `order` $\in \{1, 2, 3\}$.

Similarly, field gradients can be computed as

```
1 constexpr int order = 2;
2 double grad_x_Psi1 = sledgehamr::utils::Gradient<order>(state, i, j, k, Scalar::Psi1, dx, "x");
```

Here, the direction spatial direction can be selected through "x", "y", and "z" and we have implementations for `order` $\in \{1, 2, 3\}$ corresponding to the 3-point, 5-point, and 7-point stencil, respectively.

Appendix B: List of run-time parameters

Below is a list of all available run-time parameters including their default values, loosely separated into five different categories: `sim.*`, `amr.*`, `integrator.*`, `input.*`, and `output.*`. Additionally, we have the parameter `project.name` to select the project to run. Default values are used if the parameter has not been specified in the `inputs` file. If no default value is given, the parameter in question is mandatory and has to be added to the `inputs` file.

<code>sim.*</code>	Range	Default	Description
<code>t_start</code>	\mathbb{R}		Start time t_{start} .
<code>t_end</code>	\mathbb{R}		Final time t_{end} .
<code>L</code>	\mathbb{R}^+		Box length L .
<code>cfl</code>	\mathbb{R}^+		Sets $\Delta t_\ell / \Delta x_\ell$ for the Courant-Friedrichs-Lewy condition. This is used to derive the time step size Δt_ℓ since Δx_ℓ is uniquely determined through <code>sim.L</code> and <code>amr.coarse_level_grid_size</code> . See section II.
<code>gravitational_waves</code>	$\{0, 1\}$	0	Whether to run with gravitational waves. See section V.
<code>dissipation_strength</code>	\mathbb{R}^+	0	Sets the strength ϵ_{KO} of Kreiss-Oliger dissipation for all field components. This value will be used as a default value for all field components. If set to 0 the dissipation term will be removed. See section IID.
<code>dissipation_strength_\${ScalarField}</code>	\mathbb{R}^+	ϵ_{KO}	Sets the dissipation strength ϵ_{KO} for a particular field component by overwriting the value set by <code>sim.dissipation_strength</code> .
<code>dissipation_order</code>	$\{2, 3\}$	Null	Defines the order p of Kreiss-Oliger dissipation. The actual value corresponds to the number of ghost cells needed for the computation. This parameter needs to be set only if $\epsilon_{\text{KO}} > 0$ for any field component. See section IID.

Table I. General simulation parameters.

amr.*	Range	Default	Description
<code>coarse_level_grid_size</code>	$2^{\mathbb{N}}$		Number of cells at the coarse level in each spatial direction.
<code>max_refinement_levels</code>	\mathbb{N}		Total number of refinement levels. If set to 0 AMR will effectively be switched off.
<code>blocking_factor</code>	$2^{\mathbb{N}}$	8	The length of each box is a multiple of the blocking factor.
<code>nghost</code>	\mathbb{N}	0	Number of ghost cells. Must be smaller than the blocking factor.
<code>n_error_buf</code>	\mathbb{N}	1	Number of buffer cells during a regrid. Must be smaller than the blocking factor.
<code>regrid_dt</code>	\mathbb{R}^+	DBL_MAX	Regrid interval $\Delta t_{\text{regrid}}^{\ell=0}$ at the coarse level, where $\Delta t_{\text{regrid}}^{\ell} = \Delta t_{\text{regrid}}^{\ell=0}/2^{\ell}$.
<code>force_global_regrid_at_restart</code>	$\{0, 1\}$	0	If set to 1 a global regrid will be performed when (re-)starting a simulation instead of a local regrid. If 0, a local regrid will be attempted first.
<code>tagging_on_gpu</code>	$\{0, 1\}$	0	The cell tagging procedure during a regrid is usually done on CPUs even if GPUs are available. This is mostly to keep track of tagging statistics for diagnostic purposes. The tagging procedure is rarely a bottleneck, so not much time is wasted by running it on CPUs. However, with this toggle, we can force it to run in GPUs in lieu of collecting statistics.
<code>max_local_regrids</code>	\mathbb{N}	10	Caps the number of consecutive local regrids. If <code>max_local_regrids</code> are reached a global regrid will be performed instead and the counter resets.
<code>volume_threshold_strong</code>	\mathbb{R}^+	1.1	ϵ_s threshold during a local regrid. See section II C.
<code>volume_threshold_weak</code>	\mathbb{R}^+	1.05	ϵ_w threshold during a local regrid. See section II C.
<code>interpolation_type</code>	$\{0, 1, 2, 4\}$	4	Selects what type of spatial interpolation should be used to fill ghost cells. 0 = Piece-wise constant interpolation 1 = Linear conservative interpolation 2 = Quadratic polynomial interpolation 4 = Quartic polynomial conservative interpolation
<code>te_crit</code>	\mathbb{R}^+	DBL_MAX	Sets the TEE threshold ϵ_{ϕ} for all scalar fields. See section II B.
<code>te_crit.\$ScalarField</code>	\mathbb{R}^+	ϵ_{ϕ}	Sets the TEE threshold ϵ_{ϕ} for a particular field component by overwriting the value set by <code>te_crit</code> .
<code>semistatic_sim</code>	$\{0, 1\}$	0	Special mode where no AMR is enabled. However, each time the virtual function <code>CreateLevelIf</code> returns <code>true</code> , the entire simulation volume is refined by a factor of 2. Only the refined data is kept from there onwards.
<code>increase_coarse_level_resolution</code>	$\{0, 1\}$	0	Occasionally, it is beneficial to change the coarse level resolution. When this parameter is set to 1 the coarse level resolution is increased by a factor of 2 during the next run. For any subsequent runs, we will need to set <code>increase_coarse_level_resolution</code> back to 0 to not increase the coarse level resolution a second time and readjust the input parameters such as <code>coarse_level_grid_size</code> and <code>regrid_dt</code> accordingly.

Table II. AMR parameters.

<code>integrator.*</code>	Range	Default	Description
<code>type</code>	$\{0 - 4, 10, 20 - 22\}$		Selects the integrator type. 0 = AMReX integrator - User defined Runge-Kutta (RK) Butcher Tableau 1 = AMReX integrator - Forward Euler 2 = AMReX integrator - Trapezoid Method 3 = AMReX integrator - SSPRK3 Method 4 = AMReX integrator - RK4 Method 10 = Low-storage SSPRK3 Method (smaller memory footprint than SSPRK3) 20 = User-defined Runge-Kutta-Nyström (RKN) Butcher Tableau 21 = RKN4 Method 22 = RKN5 Method
<code>rk.weights</code>	$n \times \mathbb{R}$	Null	RK Butcher tableau weights provided as a list of values. Needed if <code>integrator.type=0</code> .
<code>rk.nodes</code>	$n \times \mathbb{R}$	Null	RK Butcher tableau nodes provided as a list of values. Needed if <code>integrator.type=0</code> .
<code>rk.tableau</code>	$n \times \mathbb{R}$	Null	RK Butcher tableau. Shall be the flattened lower triangular matrix including the diagonal. Needed if <code>integrator.type=0</code> .
<code>rkn.weights_b</code>	$n \times \mathbb{R}$	Null	RKN Butcher tableau weights \mathbf{b} provided as a list of values. Needed if <code>integrator.type=20</code> .
<code>rkn.weights_bar_b</code>	$n \times \mathbb{R}$	Null	RKN Butcher tableau weights $\bar{\mathbf{b}}$ provided as a list of values. Needed if <code>integrator.type=20</code> .
<code>rkn.nodes</code>	$n \times \mathbb{R}$	Null	RKN Butcher tableau nodes provided as a list of values. Needed if <code>integrator.type=20</code> .
<code>rkn.tableau</code>	$n \times \mathbb{R}$	Null	RKN Butcher tableau. Shall be the flattened lower triangular matrix including the diagonal. Needed if <code>integrator.type=20</code> .

Table III. Integrator settings.

<code>input.*</code>	Range	Default	Description
<code>initial_state</code>	string	""	Path to hdf5 file containing the initial state. It is also possible to provide the path to a checkpoint, in which case the level data will be initialized from the checkpoint. However, no other metadata provided by the checkpoint will be used to initialize the simulation. See section VIII.
<code>initial_state_\$\$ScalarField</code>	string	""	Path to hdf5 file containing the initial state for the scalar field <code>\$\$ScalarField</code> . See section VI.
<code>upsample</code>	$2^{\mathbb{N}}$	1	If <code>upsample > 1</code> the provided initial state will be up-scaled by the given factor. It is assumed that the provided initial state is of size <code>coarse_level_grid_size/upsample</code> .
<code>restart</code>	$\{0, 1\}$	0	If 1 we will restart the simulation from a checkpoint. By default, the latest checkpoint within the output folder will be selected.
<code>select_checkpoint</code>	string or \mathbb{N}	Null	With this parameter, we can manually select a checkpoint from which to restart the simulation. If <code>select_checkpoint ∈ ℕ</code> the corresponding checkpoint in the output folder will be used. Alternatively, <code>select_checkpoint</code> can be set to the path of a checkpoint.
<code>delete_restart_checkpoint</code>	$\{0, 1\}$	0	Defines whether we keep or delete the checkpoint from which we restarted the simulation.
<code>get_box_layout_nodes</code>	$2^{\mathbb{N}}$	0	If <code>get_box_layout_nodes > 0</code> no simulation will be performed. Instead, the coarse-level box layout will be written to an hdf5 file corresponding to the number of nodes set by this parameter. This can be used to set up an initial state split into chunks. See section VI.

Table IV. Initial state parameters.

output.*	Range	Default	Description
output_folder	string		All simulation output will be written to this path. If the folder does not exist yet it will be created.
alternative_output_folder	string	Null	A secondary output folder. It is possible to alternate output between primary and secondary output folders, see <code>output.\$OutputType.alternate</code> . This can help alleviate disk quota constraints.
rename_old_output	{0,1}	0	If the output folder already exists but we are not explicitly restarting a sim with <code>input.restart = 1</code> , then the simulation run will be aborted. This is to avoid accidentally overwriting existing simulation output. If <code>rename_old_output = 1</code> , however, the existing output folder will be renamed by adding a unique string. The simulation will then continue as normal.
output_of_initial_state	{0,1}	1	If 1, we will immediately start producing output at $t = t_{\text{start}}$. If 0, we will wait for one write interval.
write_at_start	{0,1}	0	If 1, we will immediately start producing output when restarting from a checkpoint. If 1, we will wait for one write interval since the time at which the respective output has been written last.
<code>\$OutputType.interval</code>	\mathbb{R}	-1	Sets the write interval. If negative, the respective output type will be disabled.
<code>\$OutputType.alternate</code>	{0,1}	0	If 1, the output will alternate between the primary and secondary output folders.
<code>\$OutputType.min_t</code>	\mathbb{R}	-DBL_MAX	No output will be written if $t < t_{\text{min}}$.
<code>\$OutputType.max_t</code>	\mathbb{R}	DBL_MAX	No output will be written if $t > t_{\text{max}}$.
checkpoints.rolling	{0,1}	0	If 1, only the last checkpoint is being kept on disk. Any preceding checkpoint will be deleted.
gw_spectra.projection_type	{1,2}	2	Sets the order of the projector in Eq. 15, see section VIII E.
projections.max_level	\mathbb{N}	INT_MAX	Sets the maximum level to be included in the projection output, see section VII C.
<code>\$BoxOutput.downsample_factor</code>	$2^{\mathbb{N}}$	1	All output types that save a 3D volume (<code>\$BoxOutput={coarse_box, coarse_box_truncation_error, full_box, full_box_truncation_error}</code>) can be downsampled by this factor.

Table V. Simulation output. Here, `$OutputType` is any of the following: `checkpoints`, `slices`, `coarse_box`, `full_box`, `slices.truncation_error`, `coarse_box.truncation_error`, `full_box.truncation_error`, `projections`, `spectra`, `gw_spectra`, `performance_monitor`, or `amrex_plotfile`.